Mode-shifting Minimization in a Power Management Strategy for Rapid Component Sizing of Multimode Power Split Hybrid Vehicles

2018-01-1018

Mode-shifting Minimization in a Power Management Strategy for Rapid Component Sizing of Multimode Power Split Hybrid Vehicles

Pier Giuseppe Anselma[1,3], Yi Huo[1], Joel Roeleveld[1], Edris Amin[2], Ali Emadi[1], Giovanni Belingardi[3]
[1]McMaster Institute for Automotive Research and Technology (MacAUTO), McMaster University, ON, Canada,
[2]FCA USA LLC, MI, USA, [3]Politecnico di Torino

Abstract

The production of multi-mode power-split hybrid vehicles has been implemented for some years now and it is expected to continually grow over the next decade. Control strategy still represents one of the most challenging aspects in the design of these vehicles. Finding an effective strategy to obtain the optimal solution with light computational cost is not trivial. In previous publications, a Power-weighted Efficiency Analysis for Rapid Sizing (PEARS) algorithm was found to be a very promising solution. The issue with implementing a PEARS technique is that it generates an unrealistic mode-shifting schedule. In this paper, the problematic points of PEARS algorithm are detected and analyzed, then a solution to minimize mode-shifting events is proposed. The improved PEARS algorithm is integrated in a design methodology that can generate and test several candidate powertrains in a short period of time.

Introduction

According to the EPA (US Environmental Protection Agency), 17% of Model Year (MY) 2016 vehicle production already meets or exceeds the MY 2020 CO2 emissions targets [1]: this amount is much higher than projections for earlier model years [2]. Looking ahead, however, only about 3.5% of projected MY 2016 production could meet the MY 2025 CO2 emissions targets. Vehicles meeting the MY 2025 CO2 targets are comprised solely of hybrids, plug-in hybrids, electric vehicles, and hydrogen fuel cell vehicles. As evidence, the sales of these vehicles are expected to significantly grow in the next few years.

In fact, worldwide plug-in hybrid vehicle sales for Quarter 1 (Q1) 2017 were 40% higher than for the same period in 2016 [3]. North America showed fastest growing region in Q1, with 50% growth.

Hybrid Electric Vehicles (HEVs) provide a significant potential to reduce fuel consumption and, at the same time, satisfy customer acceptance constraints [4]. Since their capability to combine the advantages of series and parallel configurations [5], power-split vehicles are the most successful and represent the largest portion of the current population of hybrid vehicles. The power-split powertrain is based on planetary gear sets (PG) which are very compact and can operate as a continuously variable transmission. Furthermore, the operation of this type of powertrain is efficient in many different vehicle categories, including Sport Utility Vehicles (SUV) [6][7] and buses [8][9].

Recently, power split transmissions have been improved with the addition of clutches in order to improve flexibility, operational efficiency and to increase the potential of the powertrain. More complex systems employ different operating modes, with each one of these best suiting a specific case of vehicle operation (i.e. launching, accelerating, cruising at high speed, regenerative braking…). By adding multimode operation fuel consumption and drivability can be improved.

The optimal design of power-split hybrid vehicles was first proposed by Liu et al. (2010), who established a systematic design approach for two planetary gear power-split two modes hybrid powertrains [10]. Based on this method, some studies have already been conducted to find the best designs using exhaustive search: Zhang et al. came up with a multimode HEV design based on the Toyota Prius where improvement in the fuel economy was achieved by including an extra clutch [11]. Bayrak et al. studied all feasible designs using a single planetary gear through the bond graph technique [12]. Zhang et al. developed an automated modeling technique for optimization of double planetary gear hybrid powertrains [13]. By improving that procedure, Zhang et al. were able to analyze the double PG powertrain used in the Chevrolet Volt Gen 2 and to propose better alternative designs based on it [14]. Recently, Zhuang et al. started analyzing hybrid powertrains with three planetary gear sets, and found they do not offer a significant fuel economy improvement compared to double planetary gear ones [27].

In this paper, we have used fuel economy as the main metric to identify the best possible configuration by using optimal energy management methodologies. In general, the energy management problem can be solved by rule-based control [16], Dynamic Programming (DP) [17][18], Equivalent Consumption Minimization Strategy (ECMS) [19][20], the Pontryagin's Minimum Principle (PMP) [21][22], and convex optimization [23]. However, since all these techniques require much time to be spent in calculation or they do not suit multi-mode powertrains, a new near-optimal energy management strategy named Power-weighted Efficiency Analysis for Rapid Sizing (PEARS) was developed, and it proved to produce optimal results similar to DP while running three to four orders of magnitude faster [24]. Although the tool is great for offline efficiency computation, the static nature of the PEARS algorithm denies it to take into account mode shift feasibility.

In a previous work by Zhang et al., an improvement was achieved by complementing the PEARS algorithm with a low-dimension DP

problem to determine the mode-shift sequence which was called PEARS+. Unfortunately, when dealing with a large pool of candidates (i.e. in the amount of 10^9) this technique could not be applied, because the computational cost of DP is still quite heavy despite the lower dimension of the problem. [25]

To overcome this computational limitation, in this paper we will propose a simpler way to enhance the PEARS algorithm in order to take into account mode-shifting frequency and to make the algorithm closer to a real-time simulation. Our intent is to develop a quick but exhaustive way to compare a very large pool of candidates in order to identify the best possible transmission configuration. Both Urban Dynamometer Driving Schedule (UDDS) and Highway Fuel Economy Test (HWFET) are taken into account for this work.

The paper is organized as follows: firstly the design methodology of double planetary gear hybrid powertrains is introduced. The procedure of PEARS algorithm is subsequently recalled. The reasons for its dis-uniformity in mode-shifting are identified and analyzed, then a solution to minimize mode-shifting is proposed. Finally, a case study and conclusions are presented.

Systematic Design Methodology

The procedure of the analytical transmission design methodology is illustrated in Figure 1 and detailed in the following paragraphs.

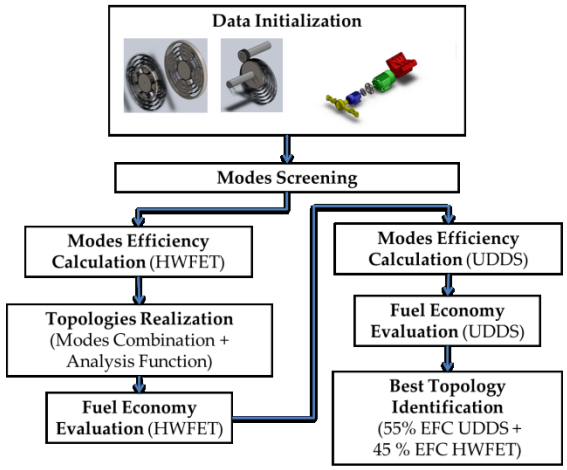

Figure 1. Flowchart of the design methodology

A. System Dynamics and Automated Modeling

Multi-mode HEVs are characterized by a planetary gear system, with additional use of clutches which are key to multiple mode operation. Focusing on a double-PG system, the total number of possible clutches is set to 16. This value is found by using equation (1) and considering the number of PG sets (N_p) equal to 2.

$$N_{clutch} = ({}_{3N_p}C_2 - 2N_p) + (3N_p - 1) \quad (1)$$

The first parenthesized term represents the possible clutches added between each pair of nodes. Since only one clutch could lock a planetary gear set by connecting any two nodes out of three in that planetary gear set, the other two ($ {}_nC_r = \frac{n!}{r!(n-r)!}$) possible connections are redundant; the second parenthesized term represents grounding clutches, all the gear nodes could be grounded except the one attached to output. Since locking any two of the three nodes in one PG produces identical dynamics, such redundant clutches are eliminated by the third term. In addition, the output shaft should not be grounded.

It should be noted that, for a specific design, if all selected modes use the same engaged clutch, that clutch can advantageously be replaced by a permanent connection.

A methodology to model the modes of multi-mode HEVs was proposed in [25]. The dynamics of any specific mode is described by the characteristic matrix A^*, as shown in equation (2). This 4x4 characteristic matrix A^*governs the relationship between the angular acceleration of powertrain devices and their corresponding torques. The detailed derivations are described by X. Zhang et al [25].

$$\begin{bmatrix} \dot{\omega}_{ICE} \\ \dot{\omega}_{OUT} \\ \dot{\omega}_{MG1} \\ \dot{\omega}_{MG2} \end{bmatrix} = A^* \begin{bmatrix} T_{ICE} \\ T_{OUT} \\ T_{MG1} \\ T_{MG2} \end{bmatrix} = \begin{bmatrix} a_{11} & a_{12} & a_{13} & a_{14} \\ a_{21} & a_{22} & a_{23} & a_{24} \\ a_{31} & a_{32} & a_{33} & a_{34} \\ a_{41} & a_{42} & a_{43} & a_{44} \end{bmatrix} \begin{bmatrix} T_{ICE} \\ T_{OUT} \\ T_{MG1} \\ T_{MG2} \end{bmatrix} \quad (2)$$

B. Mode screening, classification, and combination

Once the state-space model for a mode is obtained, the mode needs to be examined whether it is feasible. A mode is determined to be infeasible if the vehicle cannot be powered by any powertrain component, i.e., all elements of the first row of the A^* matrix are zero. Modes with the same A^* matrix are said to be identical modes.

Based on their characteristics and functionalities, each mode is divided into one of 14 different mode types shown in Table 1. Details about the criteria for the mode classification are described by X. Zhang et al [25].

A configuration is a given set of planetary gears, final drive ratio, and location of components. For every given configuration, all the possible modes are screened and their mode type is identified. Different topologies in a configuration are characterized by specific clutches and permanent connections. In addition, every possible mode can have multiple different topologies that realize the same dynamics. These topologies will be considered separately. The approach to identify the selected designs is detailed in [13]. The normalized efficiency of every mode is then calculated: the detailed explanation for this process can be found in the next section.

The need to realize some selected modes is the constraint in topologies construction. In other words, the location of clutches and permanent connections is determined by the dynamics of the modes that the topology is expected to realize.

Table 1. Unique modes for a double PG hybrid powertrain

Mode Number	Mode Type	Mode Number	Mode Type
1	Series Mode	8	ICE only (fixed gear)
2	Compound Split (3 DoFs)	9	Parallel with Fixed Gear (ICE + 2MGs, 2 DoFs)
3	Compound Split (2 DoFs)	10	Parallel with Fixed Gear (ICE + 2MGs, 1 DoF)
4	Input Split	11	Parallel with Fixed Gear (ICE + 1MG, 1 DoF)
5	Output Split	12	EV (2MGs, 2DoFs)
6	Parallel with EVT (ICE +1MG, 2 DoFs)	13	EV (2MGs, 1DoF)
7	Parallel with EVT (ICE +2MGs in serial, 2 DoFs)	14	EV (1MG, 1DoF)

This leads us to sweep all the possible pairs of modes and for each of them generate the topology that operates both of them with the minimum number of clutches. The approach to identify the locations of clutches and permanent connections is based on binary hexadecimal vectors. Details about the procedure can be found in [15].

C. Configurations Selection

Among all the possible configurations generated in the previous step, in this paper only the candidates with a maximum of 3 clutches are considered. This limits the design space to configurations that can achieve a maximum of 6 different modes.

Since the procedure so far is based on selecting only 2 modes of each candidate, the next step is the identification of all the other possible modes in each selected design. This aim is achieved through an "Analysis function", which allows shifting from the Topology Space back to the Mode Space, as shown in Figure 2. A comparison between the connections that every mode requires to be realized and the connections brought by engagements or disengagements of the clutches is made in order to identify the feasible modes of each selected configuration.

Once all the feasible modes of each configuration are detected, the next task is to test if the generated topologies are able to execute the entire driving cycle. Analyzing a specific mode, if the operating point of a component is located outside the limits of its table, that mode is considered unfeasible for that particular driving cycle point. The efficiency of the mode in the unfeasible point is marked as 0. Consequently, a configuration is kept if for all the points of the driving cycle at least one of its modes has its efficiency greater than 0, otherwise it is discarded. In this approach, the HWFET cycle is used first since its performances requirements are more restrictive than the UDDS cycle. Using this screening process, roughly 10^3 to 10^6 configurations for each specific gear parameters set are tested.

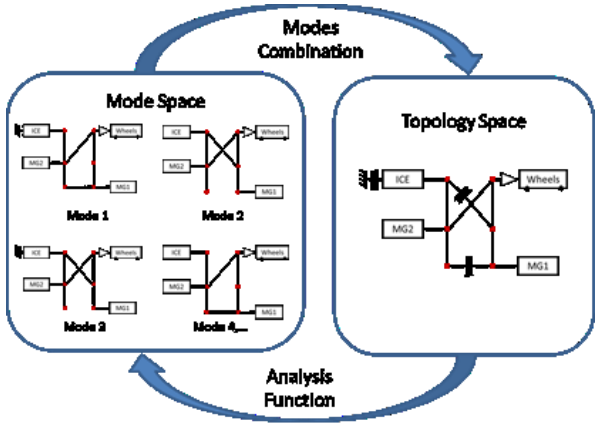

Figure 2. Transaction from topology space to mode space and vice-versa

Configuration Analysis

The configurations that have been determined capable of completing the required driving cycles are now evaluated basing on fuel economy, adopting the near-optimal control algorithm called Power-weighted Efficiency Analysis for Rapid Sizing (PEARS).

The PEARS algorithm has been shown to be the quickest method to evaluate charge balanced fuel economy, but it does not take into account at all the uniformity in the mode-shifting. As a result, the generated clutching schedules often appear to be unfeasible in the reality, due to their excessively frequent changes. An example is shown in Figure 3.

In the following paragraphs the operation of PEARS is discussed in detail with the main reasons for the unrealistic non-uniformity in mode shifting. An approach to measure the impact of mode-shifting losses in the PEARS algorithm is provided, and finally a solution on how to bring improvements in the algorithm is suggested.

A. Operation of PEARS

The process of the PEARS algorithm, which was introduced for the first time by Zhang et al. [24] and is used in this work, can be detailed as follows.

Step 1 – Target Cycle Discretization: The target cycle is time-discretized into operating points. In this paper, a different operating point is considered for each 1 second sample time of the driving cycle. The vehicle speed in the operating point is extracted and used to evaluate the acceleration and the torque demand. The collected data are then arranged into a 2-D table with vehicle speed and torque demand as the independent variables. Based on the speed and torque entries, operating point cells (OPC) are defined in the table.

Step 2 – Power-weighted Efficiency Analysis: in this step the efficiencies of EV and HEV modes are considered separately.

Step 2.1 – Analysis of EV modes: The efficiency of the EV modes is described by equation (3), where P_{EV}^{loss} includes both battery loss and electric drive loss, and P_{EV}^{in} refers to the power flowing into the system. In the driving scenario, P_{EV}^{in} is the battery power. In the braking case, this expression is the regenerative braking power. In this paper, regenerative braking is only allowed below the chassis

deceleration of 2 m/s^2, above which is considered only conventional friction to be used as stated in [26]. For modes with one DoF, all possible torque combinations (T_{MG1}, T_{MG2}) are compared and the best efficiency is recorded. For modes with 2DoF, all speed combinations $(\omega_{MG1}, \omega_{MG2})$ are also examined. The highest possible efficiency of each mode is calculated using equation (4). Meanwhile, the corresponding battery energy consumption is recorded.

$$\eta_{EV} = 1 - \frac{P_{EV}^{loss}}{P_{EV}^{in}} \quad (3)$$

$$\eta_{EV}^{*}|_{\omega_{out},\dot{\omega}_{out}} = \max[\eta_{EV}(T_{MG1}, T_{MG2})]|_{\omega_{out},T_{demand}} \quad (4)$$

Step 2.2 – Analysis of HEV modes: There are two possible power sources for hybrid modes, i.e., the engine and the battery. The power flow representation shown in Figure 4, where P_{ICE_1} is the engine power from the engine through the generator to the battery, P_{ICE_2} is the engine power that flows from the engine through the generator to the motor, P_{ICE_3} is the engine power that flows directly to the final drive. $P_{ICE\_1} + P_{ICE\_2} + P_{ICE\_3}$ is the total engine power, P_{batt} is the battery power and μ is a bit set when battery assist is required.

$$\eta_{HEV}(\omega_e, T_e) = \frac{P_{ICE\_1}\eta_G\eta_{batt}/(\eta_{ICE\_max}\eta_{G\_max})}{P_{fuel}+\mu P_{batt}} + \frac{P_{ICE\_2}\eta_G\eta_M/(\eta_{ICE\_max}\eta_{G\_max}\eta_{M\_max})}{P_{fuel}+\mu P_{batt}} + \frac{\frac{P_{ICE\_3}}{\eta_{ICE\_max}}+\mu P_{batt}\eta_{batt}\eta_M/\eta_{M\_max}}{P_{fuel}+\mu P_{batt}} \quad (5)$$

$$\eta_{HEV}^{*}|_{\omega_{out},\dot{\omega}_{out}} = \max[\eta_{HEV}(\omega_{ICE}, T_{ICE})]|_{\omega_{out},\dot{\omega}_{out}} \quad (6)$$

When the motors are delivering torque to the wheels, $P_{ICE\_1} = 0$, $P_{ICE\_2} = 0$, and no electric machine plays a role as generator. Once the battery power P_{batt} is determined, P_{ICE_3} is also determined. By sweeping T_e and ω_e, the best engine operating point is determined per equation (5). Equation (5) and (6) calculate the overall transmission efficiency by utilizing the normalized efficiency of engine and motor. The validity of this approach has been shown in papers [24][25]. Equation 6 ensures that we maximize the normalized efficiency with the least efficient component, the engine. If we maximize the normalized efficiency based on an electrified component than the engine on case will be rarely selected [25].

Engine power is selected such that total engine mechanical power P_{ICE} is fixed and the distribution among P_{ICE_1}, P_{ICE_2}, and P_{ICE_3} is only affected by the battery power. Engine efficiency $\eta_{ICE}(T_e, \omega_e)$ is the absolute engine efficiency. When engine operating points (T_e, ω_e) are swept, the maximum $\eta_{ICE}(T_e, \omega_e)$ is found for the lowest P_{fuel}. The selected engine operating point (T_e, ω_e) will be as near to the BSFC line as feasibly possible.

$$P_{ICE2} = \frac{P_M}{\eta_M \eta_G} \quad (7)$$

$$P_{ICE\_1} + P_{ICE2} = P_{Gen} \quad (8)$$

$$P_{ICE} = P_{ICE\_1} + P_{ICE2} + P_{ICE\_3} \quad (9)$$

$$P_{fuel} = P_{ICE}/\eta_{ICE} \quad (10)$$

During opportunity charging, no battery power is used for driving, $P_{batt} = 0$. The engine power sent to the battery is P_{ICE_1}. P_{ICE_2} is the only engine power going into motor(s), which is evaluated by equation (7). Once P_{ICE_2} is determined, P_{ICE_1} is calculated through equation (8). Then, P_{ICE_3} is determined with equation (9). The efficiency in equation (5) is calculated depending on different combinations of P_{ICE_1}, P_{ICE2} and P_{ICE_3} in order to find the most efficient solution. The transmission design tool evaluates HEV operation efficiencies for Series and Parallel mode operations.

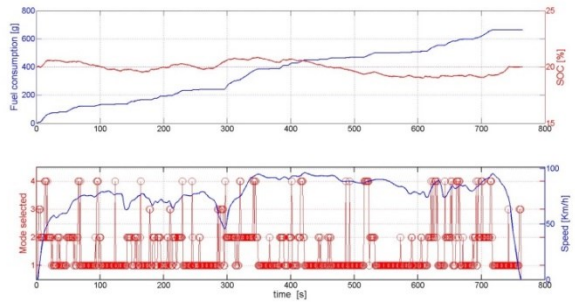

Figure 3. Fuel consumption, SOC and mode-shifting schedule obtained with original PEARS

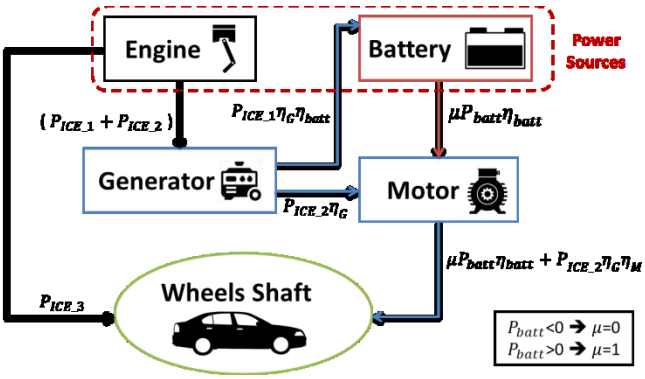

Figure 4. Power flow in the HEV mode

The power-weighted efficiency is calculated using equation (5), where P_{fuel} is the rate of fuel energy injected; subscripts G and M refer to generator (when the power is negative) and motor (when the power is positive or zero). η_{ICE_max}, η_{G_max}, and η_{M_max} are the highest efficiency of the engine, the generator, and the motors, respectively. In equation (5) both MG units' efficiencies are considered for all combination of operations: both motoring, both opportunity charging, one motoring the other opportunity charging, and both inactive.

Step 3 – Fuel Consumption Calculation and Mode Shifting Determination: Once the best power-weighted efficiencies for both EV and hybrid modes are calculated for each OPC, for the next step, it is determined whether the vehicle should operate in the hybrid or EV mode for each point of the driving cycle. Then, the expected fuel consumption (EFC) can be calculated. This step is then repeated for all the design candidates that were generated in the previous paragraphs. The flowchart of step 3 is shown in Figure 5 and the calculation involved is described as follows.

Step 3.1: The best HEV and EV modes of the candidate design are identified for each point of the driving cycle and stored in efficiency matrix. This matrix will have a row for each point of the driving cycle and 5 columns. The first column will be filled, where feasible, by the identification number of the HEV mode with the highest efficiency in that point, while the second column will contain

the value of its efficiency (η^*_{HEV}). Columns 3 and 4 will consider the best EV mode and operate as columns 1 and 2 (η^*_{EV}). The fifth column is the difference between the efficiencies of the 2 best HEV and EV modes identified ($\eta^*_{HEV} - \eta^*_{EV}$) (in other words, the difference among columns 2 and 4). An example of efficiencies matrix can be seen in Table 2.

Table 2 : Example of efficiencies matrix

Cycle Point	Best HEV mode		Best EV mode		(η_HEV - η_EV)
…	…	…	…	…	…
j-1	$mode_{HEV}^{best,j-1}$	$\eta_{j-1,mode_{HEV}^{best,j-1}}$	$mode_{EV}^{best,j-1}$	$\eta_{j-1,mode_{EV}^{best,j-1}}$	$\eta_{j-1,mode_{HEV}^{best,j-1}} - \eta_{j-1,mode_{EV}^{best,j-1}}$
j	$mode_{HEV}^{best,j}$	$\eta_{j-1,mode_{HEV}^{best,j}}$	$mode_{EV}^{best,j}$	$\eta_{j-1,mode_{EV}^{best,j}}$	$\eta_{j-1,mode_{HEV}^{best,j}} - \eta_{j-1,mode_{EV}^{best,j}}$
…	…	…	…	…	…

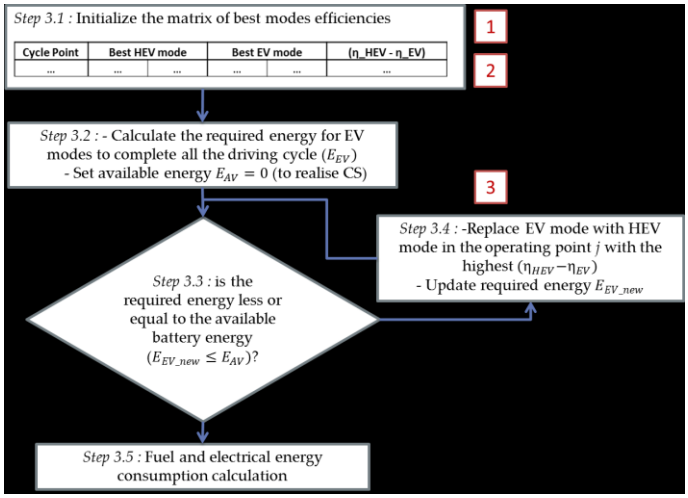

Figure 5. Flowchart of step 3

Step 3.2: First it is assumed that, if possible, all the points operate in the EV modes, and the total required energy $E_{EV}$is obtained by the sum of the battery energy consumption in each point. In this paper, the total available battery energy E_{AV} is assumed to be 0 J in order to determine whether the candidate design is able to achieve Charge Sustaining operation. In particular, the electrical energy produced during the hybrid modes operation and/or regenerative braking should be at least equivalent to the amount of electrical energy needed to complete the rest of the driving cycle in EV modes operation.

Step 3.3 – From the fifth column of the efficiencies matrix, the operating point with the highest ($\eta^*_{HEV} - \eta^*_{EV}$) is chosen (assuming it is the j_{th} point) for hybrid operation: the corresponding EV mode is replaced by the HEV mode and the required energy E_{EV} will be updated based on equation (11), where E_j^{HEV} is the battery energy (produced or consumed) in the hybrid mode

$$E_{EV\_new} = E_{EV} + E_j^{HEV} - E_j^{EV} \qquad (11)$$

Meanwhile, the fuel consumption in the j_{th} point is recorded. The j_{th} row in the efficiencies matrix is then filled with 0 to not consider the j_{th} point anymore in the replacement process.

Step 3.4 – Step 3.3 is repeated until E_{EV} is less than or equal to E_{AV}, thus it is null or negative. If, after looping all the possible points, E_{EV} is still greater than E_{AV}, this indicates that the current design candidate is not capable of finishing the cycle charge balanced and it will be marked as an infeasible design.

Step 3.5 – After determining the points that will operate in the hybrid mode, the EFC is evaluated by the sum of the fuel consumption in the points replaced by hybrid operation.

Step 3.6 – Steps 2 and 3 are repeated for each sizing design candidate, until all sizing parameters are determined. The design with the lowest EFC is recorded as the optimal configuration for the corresponding candidate.

B. Sources of non-uniformity in mode-shifting for PEARS

After applying the PEARS algorithm, the mode-shifting sequence along with the evaluation of the fuel consumption and the State of Charge (SOC) of the battery can be completed for the entire driving cycle.

The mode-shifting sequence solved by the PEARS algorithm is often found to be infeasible. This is due to the frequent and sudden changes in the selected mode. Analyzing the structure of the algorithm, three main sources of non-uniformity in mode shifting can be identified and described as follows. Their position in the flowchart of the algorithm is shown by the corresponding number in Figure 5.

1. In the initialization of both EV and HEV modes sequence (reported in the efficiencies matrix), sometimes a HEV mode appears to be more efficient than the second most efficient HEV mode for just 1 operating point, despite the narrow range between their efficiencies. The same can be observed for the EV modes.
2. For some operating points, only HEV modes are feasible, while only EV modes are feasible for other points. For example, compound split HEV modes are the only ones that can achieve high accelerations, while only EV modes can operate in mild-strong regenerative braking situations. Even in these cases we may be obliged to use a mode for 1 or a few operating points, while other modes are used in the other close points due to a narrow range between efficiencies.
3. A main source of non-uniformity in mode shifting lies in the point-by-point operation of the PEARS algorithm. This makes the substitution process able to jump from an operating point to another one located far from the previous in the driving cycle.

C. Mode shifting loss measurements

In the previous paragraph we identified the sources of mode shifting non-uniformity, but we still need a way to measure their impact on the powertrain operation.

A cost function can be used to apply a penalty every time a mode shifting occurs in the driving cycle. Mode shifting requires the engagement or disengagement of clutches, which cause mechanical losses in the transmission. The DP technique involves an iterative process to minimize a similar cost function in the mode-shifting sequence. In this work, the accumulated penalty is considered for a configuration only as an indicator to estimate the impact of the non-

uniformity in mode-shifting. The penalty added by the original PEARS algorithm will be compared to the calculated penalty after the improvement of the algorithm to prove the reduction.

In this paper we consider that every time a shift occurs (i.e. from the *ii* point to the *ii+1* point), 10 % of the power generated or received by the components (ICE, MG1 and MG2) in the *ii* and the *ii+1* points is lost. This value does not really represent an estimation of the real losses of the transmission, rather it is considered as a hypothetical value. The observed penalty is calculated using equation (12) below.

$$penalty = 10\,\% * \left(\frac{P_{out,ii_{point}}}{\eta_{mode\ ii_{point}}} + \frac{P_{out,ii+1_{point}}}{\eta_{mode\ ii+1_{point}}}\right) \quad (12)$$

Where P_{out} is the output power to the road through the axle and wheels from the powertrain, and η_{mode} is the total efficiency of the mode used in the *ii* or the *ii+1* point of the driving cycle.

A configuration with 3 clutches can operate with a maximum of 6 different modes, thus for each candidate the penalty of the cost function can be represented by a square matrix whose dimension is equal to the configuration's number of modes. Each mode shows up both in the rows and the columns, where the rows represent the mode in the *ii* point and the columns represent the mode in the *ii+1* point. The main diagonal of the matrix is populated by zeros since there is no penalty if the mode-shifting does not occur, whereas the zeros outside the main diagonal indicate that a mode is unfeasible in the *ii* or in the *ii+1* point. An example of a cost function matrix is represented in Figure 6.

D. Mode shifting loss minimization process

The main goal is to apply the PEARS algorithm shifting the operating mode only when essential, while finding the solution that represents the minimum fuel consumption. In other words, a more realistic mode-shifting sequence is likely to be obtained.

First, the threshold range between efficiencies below which a mode can be kept for more than one operating point is determined. To better explain this concept the example Table 3 is shown. Mode 2 appears to have a higher efficiency only in the j_{th} point, despite the narrow difference between the efficiencies of the two modes. Thus keeping mode 1 in the j_{th} point on one hand would not cause a large increase in the fuel consumption, while on the other hand it would benefit the uniformity in the mode-shifting sequence.

The threshold value for the difference in efficiencies should create the most uniform mode-shifting sequence, but at the same time it should not cause a large decrease in the overall efficiency of the powertrain operation. Testing a sample of configurations generated from a hundred different locations of components revealed this threshold value should be 90 % of the best mode efficiency. The test was completed by gradually decreasing (1 % every time) the threshold value in the procedure described until the desired operation was achieved.

In order to minimize the mode-shifting, a method to reduce the mode changes is proposed by the motivations for non-uniformity identified in the previous paragraph. Figure 10 in Appendix 1 shows the flowchart of *step 3* of the improved algorithm, with the additional steps marked in red.

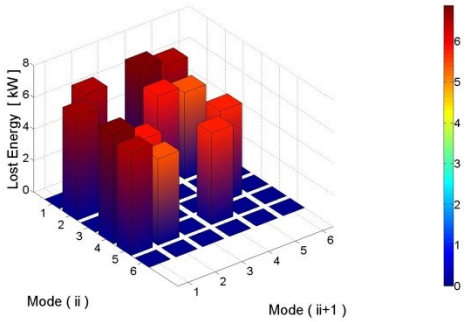

Figure 6. Example of a cost function matrix

Table 3. Example of modes efficiencies for adjacent operating points

Cycle Point	η_HEV mode 1	η_HEV mode 2
…	…	…
i	0.998	0.988
j	0.992	0.993
k	0.994	0.992
…	…	…

1. In the initialization of the sequences of the best HEV modes, if during the j_{th} point the efficiency of the HEV mode selected in the $j_{th} - 1$ point is greater than the 90 % of the efficiency of the best HEV mode in the j_{th} point, then in the j_{th} point the same HEV mode of the previous point is kept. The same procedure is then used to initialize the sequence of the best EV modes (*step 3.1.1*).
2. The procedure of *step 3.3* begins by selecting hybrid operating points in which only hybrid modes are feasible (*step 3.2.1*). This mandatory criterion is taken into account in order to allow the candidate design to complete the entire driving cycle. After all these points are replaced, priority is given for hybrid operation to the points next to the previously considered ones. In other words, the efficiency of the hybrid modes at all the points are examined immediately before or after the already replaced points. The highest $(\eta^*_{HEV} - \eta^*_{EV})$ value is selected among these points and the corresponding point is selected for hybrid operation.
   Automatically, the points immediately before and after the previously replaced points are taken into account in the group of considered points. As a matter of fact, the single driving cycle point is turned into a range of hybrid operation points where possible. The procedure is repeated until the hybrid mode replacement is infeasible in the extreme points of each range, or it causes an excessive drop in the efficiency (efficiency smaller than the 90 % of the efficiency of the best mode in the considered operating point) (*step 3.3.1*).
3. During the process described in *step 3.3*, after the first replacement of hybrid operation point (j_{th}), for the following substitution priority is given to the points next to the previously replaced one. If the efficiency of the previously selected HEV mode in the point $(j_{th} - 1)$ or in the point $(j_{th} + 1)$ is greater than the 90 % of the efficiency of the best HEV mode in one of those points, the selected HEV mode is used in one of the adjacent points (*step 3.3.2*).

Mode-shifting minimization is obtained by converting the operation point-by-point in this way.

E. Mode shifting loss comparison and results

Figure 7 (a) shows an example of a possible components location belonging to a vehicle whose parameters are illustrated in Table 4. Considering HWFET cycle only, an optimal design is first identified using the original PEARS algorithm and showed in Figure 7 (b). Its mode-shifting sequence is illustrated in Figure 3.

After repeating the calculation with the improved PEARS algorithm, the detected optimal design is different from the previous one and shown in Figure 7 (c). The obtained new mode-shifting sequence is shown in Figure 8. The fuel consumption, the obtained penalty, and the computation time required given the same computer to identify the best design for the data are shown for both topologies in Table 5.

The results show that the identified optimal design can change by using the algorithm with the proposed changes, and the optimal fuel consumption increases as expected. As an interpretation, the original optimal design is more heavily penalized than the increase of fuel consumption for the new optimal design. Therefore, the original optimal design suffered from very frequent mode-shifting, while the increase in fuel consumption of the new optimal design is less than 2% in this case. The large reduction of the penalty (the new one is less than 5% of the original one) indicates the achievement of a much more uniform mode-shifting sequence, as shown in Figure 8. Furthermore, no substantial increase can be observed in the computation time.

In conclusion, the improved algorithm can find the optimal solution while applying mode-shifting only when strictly necessary.

Once the study parameters and the location of components are set, the mode screening process is completed, the candidate topologies are realized and the correspondent modes are identified, the optimal design can be detected for fuel consumption. Both UDDS and HWFET cycles are simulated, and the weighted average (55/45) [28] is used to represent the combined fuel consumption of the designs.

Among the 66 candidates that meet all the requirements and are obtained with the given parameters, the optimal design results are shown in Figure 9. Only 35 minutes are required to execute the entire process shown in Figure 1 on a desktop computer with Intel i5-2400S (2.5 GHz) and 8 GB RAM.

Furthermore, changing the input parameters and repeating the procedure could quickly enable parameter optimization (planetary gear and final drive ratios, component locations, component sizing, and clutch connections).

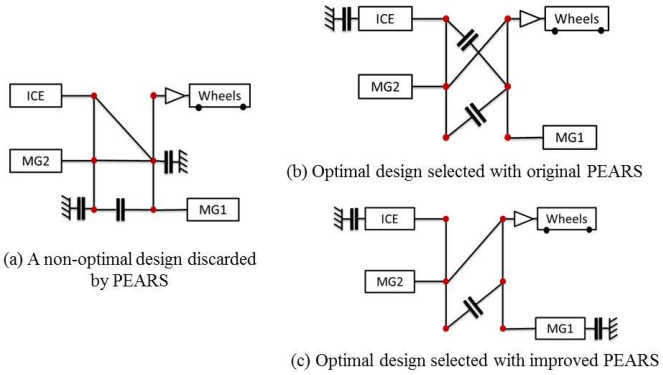

(a) A non-optimal design discarded by PEARS

(b) Optimal design selected with original PEARS

(c) Optimal design selected with improved PEARS

Figure 7. Identified HWFET optimal designs

Table 4. Parameters of the vehicle used in the study

Component	**Parameters**
Engine	188 kW @ 5800 rpm 320 Nm @ 4400 rpm
$P_{MG1_{max}}[kW]$	60
$P_{MG2_{max}}[kW]$	85
Final Drive Ratio	3.59
R_1: S_1	1.6
R_2: S_2	2.4
Vehicle Mass [kg]	2248

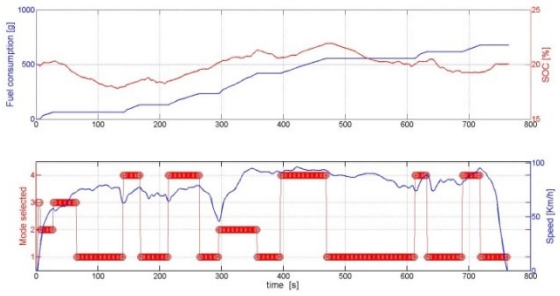

Figure 8. Fuel consumption, SOC and mode-shifting schedule obtained with improved PEARS

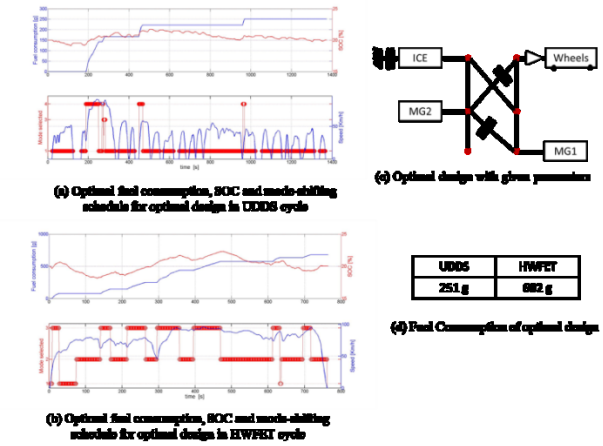

Figure 9. Optimal design research results

Table 5. Comparison parameters between algorithms

	Original PEARS	Improved PEARS
Fuel Consumption [g]	662	675
Mode Shift Penalty [kJ]	722,61	27,38
Calculation time [sec]	102	104

Conclusions

A systematic design methodology for double PG power-split hybrid powertrains via mode combination, based on previous modeling techniques, is introduced. Several possible candidates can be analyzed with the target of improving fuel economy.

The PEARS algorithm has been used as a near-optimal control strategy, but the obtained non-uniform mode-shifting schedule reveals to be infeasible. A study of the steps that bring non-uniformity in mode-shifting during the procedure is completed. Based on the analysis, some corrections are proposed to be applied to the algorithm to realize mode-shifting only when it is necessary.

The impact of the algorithm corrections is found to be more than 20 times the reduction of losses measured through a cost function. On the other hand, the increase in fuel consumption is contained within 2%.

The improved algorithm reveals itself as a good way to check the feasibility of the candidate designs and to realize uniform mode-shifting schedules. This target is achieved without recurring to DP, which is found to have a heavy computational cost.

Contact Information

Pier Giuseppe Anselma, Department of Mechanical and Aerospace Engineering (DIMEAS), Politecnico di Torino, Corso Duca degli Abruzzi 24, 10129 Torino, Italy. Mail: pganselma@gmail.com

Acknowledgments

This research was completed, in part, thanks to funding from the Canada Excellence Research Chairs (CERC) Program, Natural Sciences and Engineering Research Council of Canada (NSERC), Automotive Partnership Canada (APC) Initiative, along with the industrial partners FCA US LLC, and FCA Canada Inc.

References

1. Light-Duty Automotive Technology, Carbon Dioxide Emissions, and Fuel Economy Trends Report Overview. [Accessed Jan. 23, 2017]. [Online], https://www.epa.gov/fuel-economy/trends-report
2. J. M. Miller, A. Emadi, A. V. Rajarathnam, and M. Ehsani, "Current status and future trends in more electric car power systems," in *Proc. 1999 IEEE Vehicular Technology Conference*, Houston, TX, May 1999, pp. 1380–1384.
3. Global Plug-in Sales for 2017 Q1 + April [Accessed August 23, 2017]. [Online], http://www.ev-volumes.com/news/global-plug-in-sales-for-2017-q1-april/
4. A. Emadi, K. Rajashekara, S. Williamson, S. Lukic, "Topological Overview of Hybrid Electric and Fuel Cell Vehicular Power System Architectures and Configurations," *IEEE Transactions on Vehicular Technology*, vol. 54, no. 3, pp. 763-770, 2005.
5. S. M. Lukic and A. Emadi, "Effects of drivetrain hybridization on fuel economy and dynamic performances of parallel hybrid electric vehicles," *IEEE Transactions on Vehicular Technology*, vol. 53, pp. 385–389, Mar. 2004
6. I. J. Albert, E. Kahrimanovic, and A. Emadi, "Diesel Sport Utility Vehicles With Hybrid Electric Drive Trains," *IEEE Transactions on Vehicular Technology*, vol. 53, No. 4 pp. 1247–1256, July 2004.
7. S. S. Williamson and A. Emadi, "Comparative assessment of hybrid electric and fuel cell vehicles based on comprehensive well-to-wheels efficiency analysis," *IEEE Transactions on Vehicular Technology*, vol. 54, no. 3, pp. 856-862, May 2005.
8. S. S. Williamson, S. G. Wirasingha, and A. Emadi, "Comparative Investigation of Series and Parallel Hybrid Electric Drive Trains for Heavy-Duty Transit Bus Applications," in *Conf. IEEE-VPPC*, 2006, pp. l-l0.
9. E.Azzouzi, M. Iuliano, F. Camargo-Rosa, S. Patalano, M. Hammadi, O. Veneri, C. Capasso, "Systems Engineering Approach for eco-comparison among power-train configurations of hybrid bus," in *Systems Conference (SysCon)*, 2016 Annual IEEE.
10. J. Liu and H. Peng, "A systematic design approach for two planetary gear split hybrid vehicles," *Vehicle System Dynamics*, vol. 48, pp. 1395-1412, 2010.
11. X. Zhang, C. Li, D. Kum, and H. Peng, "Prius+ and Volt-: Configuration analysis of power-split hybrid vehicles with a single planetary gear," *IEEE Transactions on Vehicular Technology*, vol. 61, no. 8, pp. 3544–3552, Oct. 2012.
12. A. Bayrak, Y. Ren, P. Papalambros, "Design of Hybrid-Electric Vehicle Architectures Using Auto-Generation of Feasible Driving Modes," in *ASME Int. Design Eng. Tech. Conf. and Comput. and Inform. In Eng.Conf.*, 2013, pp. V001T01A5-VT01A5.
13. X. Zhang, H. Peng, J. Sun, S. Li, "Automated Modeling and Mode Screening for Exhaustive Search of Double-Planetary-

Gear Power Split Hybrid Powertrains." in *ASME Dynamic Syst. and Control Conf.*, San Antonio, Texas, 2014, pp. V001T15A2-VT15A2.
14. X.Zhang, S.E. Li, H. Peng, J. Sun, "Design of Multimode Power-Split Hybrid Vehicles-A Case Study on the Voltec Powertrain System", *IEEE Transactions on Vehicular Technology*, vol. 65, no. 6, pp. 4790-4801, 2016.
15. W. Zhuang, X. Zhang, H. Peng, L. Wang, "Rapid Configuration Design of Multiple-Planetary-Gear Power-Split Hybrid Powertrain via Mode Combination", *IEEE/ASME Transactions on Mechatronics*, vol. 21,no. 6, pp. 2924 - 2934 , 2016.
16. Y. Wang, Z. Sun, "Dynamic Analysis and Multivariable Transient Control of the Power-Split Hybrid Powertrain," *IEEE/ASME Transactions on Mechatronics*, vol.20, no.6, pp.3085-3097, 2015.
17. A. Sciarretta, M. Back and L. Guzzella, "Optimal Control of Parallel Hybrid Electric Vehicles," *IEEE Transaction on Control System Technoly*, vol. 12, no. 3, pp. 352-363, 2004.
18. Q. Gong, Y. Li and Z.R. Peng, "Trip-Based Optimal Power Management of Plug-in Hybrid Electric Vehicles", *IEEE Transactions on Vehicular Technology*, Vol. 57, No. 6, pp. 3393-3401, November 2008.
19. C. Musardo, G. Rizzoni, Y. Guezennec and B. Staccia, "A-ECMS: An Adaptive Algorithm for Hybrid Electric Vehicle Energy Management," *European J. of Control*, vol. 11, no. 4-5, pp. 509-524, 2005.
20. A. Sciarretta, M. Back, and L. Guzzella, "Optimal control of parallel hybrid electric vehicles," *IEEE Transactions on Vehicular Technology*, vol. 12, no. 3, pp. 352–363, May 2004.
21. S. Delprat, J. Lauber, T. M. Guerra, and J. Rimaux, "Control of a parallel hybrid powertrain: Optimal control," *IEEE Transactions on Vehicular Technology*, vol. 53, no. 3, pp. 872–881, May 2004.
22. S. Delprat, T. M. Guerra, and J. Rimaux, "Control strategies for hybrid vehicles: Optimal control," in *Proc. 56th IEEE Vehicular Technology Conference*, May. 2002, pp. 1681–1685
23. T. Nüesch, P. Elbert, M. Flankl, C. Onder and L. Guzzella, "Convex Optimization for the Energy Management of Hybrid Electric Vehicles Considering Engine Start and Gearshift Costs," *Energies*, vol. 7, no. 2, pp. 834-856, 2014.
24. X. Zhang, H. Peng, J. Sun, "A near-optimal power management strategy for rapid component sizing of power split hybrid vehicles with multiple operating modes," in *American Control Conference(ACC)*, 2013, pp.5972-5977.
25. X. Zhang, S. Li, H. Peng, J. Sun, "Efficient Exhaustive Search of Power Split Hybrid Powertrains with Multiple Planetary Gears and Clutches," *J. of Dynamic Syst., Measurement, and Control*, vol. 137, no. 12, 2015.
26. A. Emadi, "Advanced Electric Drive Vehicles", CRC Press 2014, Print ISBN: 978-1-4665-9769-3, Chapter 11. "Fundamentals of Hybrid Electric Powertrains"
27. W. Zhuang, X. Zhang, Y. Ding, L. Wang, X. Hu, "Comparison of multi-mode hybrid powertrains with multiple planetary gears", *Applied Energy*, 2016, vol. 178, issue C, pages 624-632
28. Gasoline Vehicles: Learn More About the New Label. [Online]. Available: https://www.fueleconomy.gov/feg/label/learn-more-gasoline-label.shtm

Appendix 1

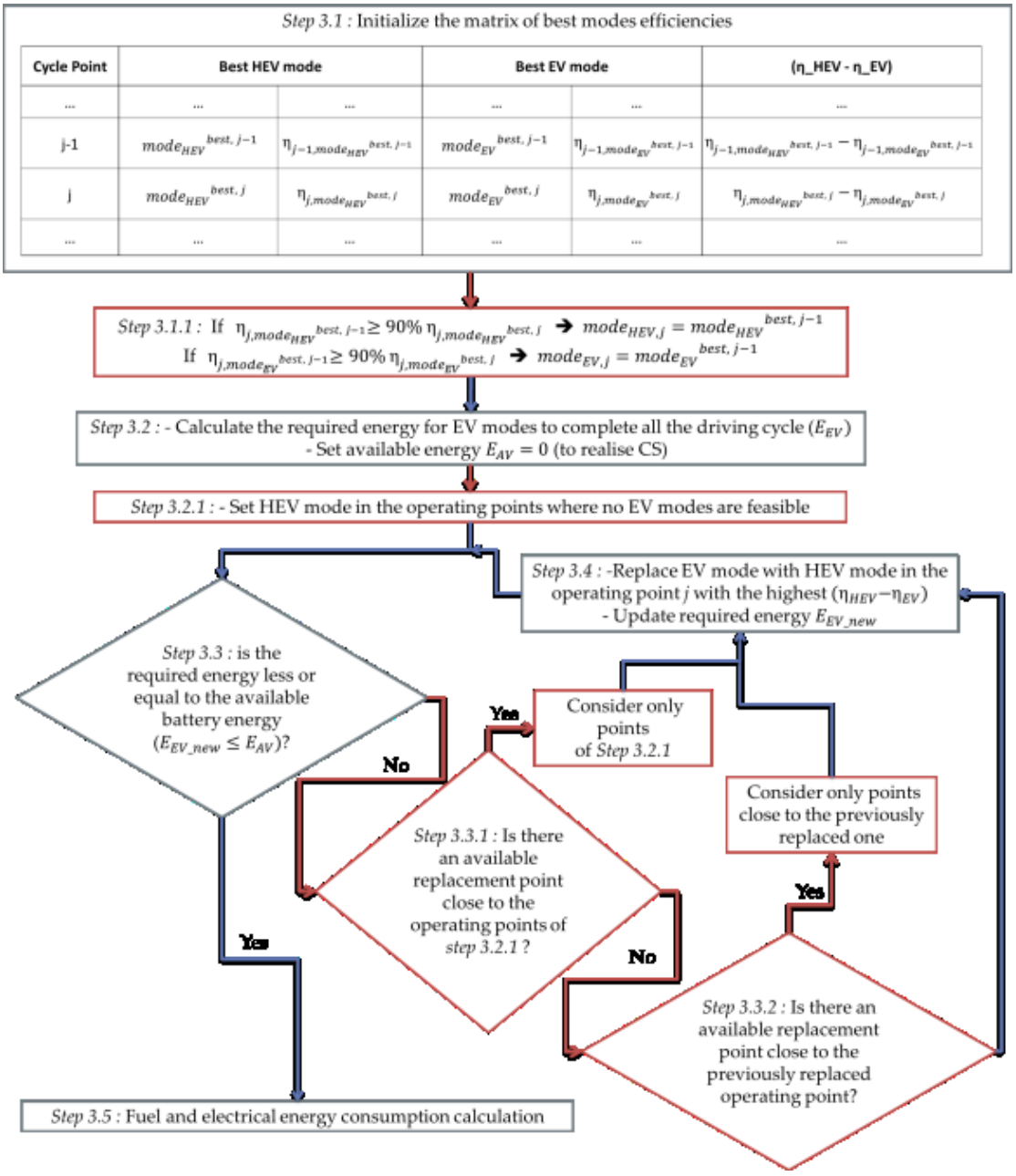

Figure 10 : Flowchart of step 3 of the improved PEARS